

Ismaël Lajaaïti, Sophia Lambert, Jakub Voznica, H       Morlon, Florian Hartig

could be used in this case as a likelihood-free inference technique. Here, we explore this idea in more detail, with a particular focus on understanding the ideal network architecture and data representation for using DL in phylogenetic inference. We evaluate the performance of different neural network architectures (DNN, CNN, RNN, GNN) and phylogeny representations (summary statistics, Lineage Through Time or LTT, phylogeny encoding and phylogeny graph) for inferring rates of the Constant Rate Birth-Death (CRBD) and the Binary State Speciation and Extinction (BISSE) models. We find that deep learning methods can reach similar or even higher accuracy than Maximum Likelihood Estimation, provided that network architectures and phylogeny representations are appropriately tuned to the respective model. For example, for the CRBD model we find that CNNs and RNNs fed with LTTs outperform other combinations of network architecture and phylogeny representation, presumably because the LTT is a sufficient and therefore less redundant statistic for homogenous BD models. For the more complex BiSSE model, however, it was necessary to feed the network with both topology and tip states information to reach acceptable performance. Overall, our results suggest that deep learning provides a promising alternative for phylogenetic inference, but that data representation and architecture have strong effects on the inferential performance.

41

Keywords: Cladogenesis, Machine Learning, Macroevolution, Stochastic Biodiversity Model

44

45

46

47

DEEP LEARNING TO INFER PHYLOGENY PARAMETERS

48

INTRODUCTION

49 Species richness varies greatly across taxonomic groups (G. E. Hutchison
50 1959), geological times (Barnosky et al. 2011) and geographical regions (Gaston
51 and Blackburn 2000). It is generally accepted that these patterns in species richness
52 emerge from variation in speciation and extinction rates in addition to dispersal and
53 migration processes. For instance, important ecological phenomena such as the
54 ‘Latitudinal Diversity Gradient’ (Hillebrand 2004) may be partly explained by
55 variations in species net diversification rates defined as the balance of the speciation
56 and the extinction rate (Mittelbach et al. 2007; Rolland et al. 2014; Pontarp et al.
57 2019). Our general understanding of the processes that cause these rates changes,
58 however, is still very limited (Rabosky 2009a, 2009b; Condamine et al. 2013; Moen
59 and Morlon 2014).

60 To better understand the drivers of variation in diversification rates and their
61 consequences for biodiversity dynamics, it is crucial first to accurately estimate net
62 diversification rates (Pyron and Burbrink 2013), and then decompose them into
63 speciation and extinction rates (Stadler 2013). The latter is not trivial, as fossil data
64 are rarely available and reconstructed phylogenies do not include information on
65 extinct species. Indeed, without further constraints, the problem is ill-posed, meaning
66 that different diversification dynamics can lead to the same extant phylogeny (Louca
67 and Pennell 2020; Morlon et al. 2022). However, when making additional
68 assumptions about the functional form of extinction and speciation rates over time, it
69 is often possible to statistically estimate the parameters of these functions, and thus
70 infer the path that led to the currently observed species (Nee et al. 1994; Etienne
71 and Rosindell 2012; Morlon 2014).

Ismaël Lajaaïti, Sophia Lambert, Jakub Voznica, H  l  ne Morlon, Florian Hartig

Arguably one of the simplest diversification models is the Constant Rate Birth-Death (hereafter 'CRBD') model, which assumes that the speciation and extinction rates are both homogeneous across lineages and constant through time. Nee et al. (1994) showed that extinction and speciation rates in this model can be estimated based on reconstructed phylogenies with Maximum Likelihood using a distinct pattern called the "pull of the present". In recent years, many studies have worked on extending this model to account for various types of rate heterogeneity as well as their potential drivers (Morlon et al. 2011; Etienne et al. 2012). These models commonly allow for variations of speciation and extinction rates through time (time-dependent models), across lineages (inhomogeneous models) as well as in dependence of environmental (Condamine et al. 2013) or biotic factors (Etienne et al. 2012). For instance, the time dependent Birth-Death model (Hallinan 2012) allows to consider homogenous changes (e.g. an exponential decay) of speciation and extinction rates over time (Rabosky and Lovette 2008; Morlon et al. 2011; Stadler 2011). Other diversification models allow lineage-specific shifts in diversification rates that can be either discrete, as can be expected to occur with the appearance of key innovations (Alfaro et al. 2009), or continuous, as can be expected to occur given the gradual evolution of phenotypes (e.g. the 'ClADS' model; Maliet et al. 2019). The specific innovations or phenotypes that drive these shifts can be either implicit, as in the latter models, or explicitly modeled, as in State-dependent Speciation and Extinction (SSE) models. A particular example of this is the Binary State Speciation and Extinction model, hereafter 'BiSSE' (Maddison et al. 2007), which considers the effect of a binary state on speciation and extinction rates.

A constant challenge when developing new diversification models is establishing robust methods to fit them to data. For diversification models with low or

DEEP LEARNING TO INFER PHYLOGENY PARAMETERS

moderate complexity, the likelihood (*i.e.* the probability to observe a reconstructed phylogeny given the model and its parameters) can be computed analytically or approximated numerically (see Nee et al. 1994 for the CRBD model and Maddison et al. 2007 for the BiSSE model). If the likelihood can be computed, model parameters can be inferred using either Maximum Likelihood Estimation (MLE; see for instance Ricklefs 2007) or Bayesian inference (*e.g.* Silvestro et al. 2011).

When the likelihood of a diversification model is analytically or numerically intractable, simulation-based methods such as Approximate Bayesian Computation (ABC) are typically being used. The ABC approach approximates the likelihood of a model by comparing model predictions to data via summary statistics (Csilléry et al. 2010; see Saulnier et al. 2017 for an example). Although ABC can successfully infer parameters from complex diversification models, it has two major drawbacks. First, ABC typically requires a large number of simulations, which is often computationally prohibitive in practical applications. Secondly, ABC suffers from the curse of dimensionality, meaning that the computational increases sharply with the dimensions of the summary statistics, which must be at least as large as the number of model parameters to ensure sufficiency (Beaumont 2010; Csilléry et al. 2010; Hartig et al. 2011). Together, both properties limit the applicability of ABC to complicated models with many parameters.

Recent advances in the field of deep learning algorithms provide an alternative for likelihood-free inference in phylogenetic inference. Unlike ABC, deep learning can easily deal with high-dimensional data and even benefit from it (LeCun et al. 2015), thus avoiding the necessity to find appropriate summary statistics. It was shown that deep learning approaches based on Convolutional Neural Networks (CNNs) can outperformed ABC for inference tasks in population genomics (Chan et al. 2018;

Ismaël Lajaaïti, Sophia Lambert, Jakub Voznica, H       Morlon, Florian Hartig

Schrider and Kern 2018). Moreover, as pointed out by (Schrider and Kern 2018), neural networks are very flexible about their input data structure, possibly allowing a far greater or more diverse set of inputs than in traditional statistical models.

Unlike for ABC, however, there is little experience on using deep learning algorithms for parameter inference in diversification models, and there are a number of options to implement DL for phylogenetic inference. One of the first questions to solve is how to best encode phylogenetic data, which in turn affects the DL architectures that could be considered for training. Recently (Voznica et al. 2022) developed a full matrix representation for non-ultrametric phylogenies with the goal of fitting epidemiological models, and compared the performance of feed-forward neural networks (DNNs) and CNNs that were supplied either with this tree representation or with conventional summary statistics to likelihood-based inference techniques. (Lambert et al. 2022) adapted this approach with the goal of fitting birth-death diversification models to reconstructed (ultrametric) phylogenies, extended the matrix representation to the case of representing phylogenies with associated tip state data, and similarly compared the performance of DNN, CNN and MLE. These studies showed that the matrix encoding processed by CNNs performed very well, leading to gains in predictive performance compared to likelihood-based methods (Voznica et al. 2022). However, there are a number of further options regarding the encoding and the network architectures, and we conjectured that the optimal combinations of those would depend on the diversification model to be estimated.

When considering the choice of network architecture (Pichler and Hartig 2023), the simplest option would be a standard fully connected Deep Neural Network (DNN). The disadvantage of this option is that fully connected DNNs do not perform favorably with high-dimensional structured input data (such as phylogenies).

DEEP LEARNING TO INFER PHYLOGENY PARAMETERS

Therefore, we can anticipate for successfully using DNNs, we would have to summarize the phylogeny's shape (which by default is high dimensional with neighborhood relationships being represented as a graph) using a limited number of summary statistics (Saulnier et al. 2017), similar to the ABC approach. While possible, this might result in a loss of information for the inference, depending on whether those summary statistics are sufficient for the inference task.

A second option would be the use of Convolutional Neural Networks (CNNs). CNNs apply one or several filters that slide incrementally across the input data to detect spatial patterns. CNNs have shown great success for a variety of tasks, including for fitting birth-death models to pathogen or species phylogenies encoded in a full matrix representation (Voznica et al. 2022; Lambert et al. 2022). CNNs could also be used on reduced representations of the phylogeny, such as the Lineage Through Time (hereafter 'LTT') plot. This seems promising as it is known that the slope of the LTT is a sufficient statistics for homogeneous models (Nee et al. 1994; Ricklefs 2007).

When representing the phylogeny by its LTT, another option is the use of Recurrent Neural Networks (RNNs). The neurons of RNNs include a temporal feedback and, thanks to this feature, RNNs can process sequential data (e.g., time series) more efficiently. A common and efficient RNN neuron architecture is the Long Short-Term Memory (LSTM) cell. RNNs based on LSTM cells can flexibly handle long and short term dependencies of the input data (Hochreiter and Schmidhuber 1997; Yu et al. 2019) and have been applied with success in many fields, including Natural Language Processing tasks (Huang et al. 2019), financial market forecasting (Bukhari et al. 2020) or phoneme classification (Graves et al. 2005).

Ismaël Lajaaïti, Sophia Lambert, Jakub Voznica, H       Morlon, Florian Hartig

Finally, when considering the nature of a phylogeny, Graph Neural Networks (GNNs) arise as a natural choice. GNNs generalize the idea of CNNs, which require Euclidean neighborhoods, to graphs (Scarselli et al. 2009; Zhang et al. 2019; Wu et al. 2021). GNNs are successfully used for many applications with a graph structure, e.g. predicting molecules properties (Gilmer et al. 2017; Mansimov et al. 2019). The potential advantage of using GNNs over CNNs is that GNNs can directly perform convolutions along the phylogeny's topology, whereas the use of a CNN requires transforming the phylogeny into a Euclidean structure, which potentially distorts neighborhood relationships.

The hypotheses formulated in the previous paragraphs are based on the theoretical knowledge about DL architectures, but so far, no systematic comparison of the combination of phylogeny representation and neural network architecture has been performed to confirm these conjectures. For example, while CNNs feeding on encoded phylogenies were shown to infer rates with a good accuracy for different birth-death models (Voznica et al. 2022; Lambert et al. 2022), we might expect that this full encoding is redundant and thus suboptimal for homogeneous birth-death models, because for these models, all the relevant information is in the LTT (Lambert and Stadler 2013).

In this study, we systematically explore the interplay between model, data representation and network architecture when inferring parameters of diversification models using deep learning. As models, we considered the simple homogeneous CRBD model and the more complex inhomogeneous BiSSE model, with the idea that homogenous diversification models will require other data representations than inhomogeneous models. We represented phylogenies with either: LTTs, sets of summary statistics, phylogeny encodings from (Voznica et al. 2022 and Lambert et

DEEP LEARNING TO INFER PHYLOGENY PARAMETERS

al. 2022), or phylogeny graphs. Then, these representations were combined with the suitable neural network architecture(s): summary statistics with DNNs, phylogeny graphs with GNNs, encoded phylogenies with CNNs, and LTTs with CNNs or RNNs. To evaluate the predictive performance of these deep learning inference methods, we compared the prediction errors of each method and broke them down into three terms: 1) variance, 2) uniform bias and 3) consistency bias (Smith and Rose 1995). As a reference, we compared the deep learning results to the MLE for these models, which is tractable in both cases.

Using this set-up, we ask three questions. First, can deep learning methods accurately infer rates from diversification models, as suggested by (Lambert et al. 2022), and if so, can these methods outperform MLE regarding the prediction error? We hypothesize that deep learning methods can theoretically outperform MLE as they can trade off bias against variance to minimize the total error. Secondly, what is the optimal representation of phylogeny data to infer rates for diversification models of different complexity? We expect, for example, that the LTT is a sufficient statistic for simple homogeneous models and is often preferable due to its simplicity. For more complex models and specifically for inhomogeneous models, on the other hand, we expect that simple representations such as the LTT will fail to provide the neural network with the necessary information. More complex representations are necessary for optimal inferential performance. Lastly, we ask how the choice of the neural network architecture in combination with the chosen phylogeny representation affects the inference. We hypothesize that the more complex the phylogeny representation, the more important the neural network architecture becomes.

METHODS

Ismaël Lajaaïti, Sophia Lambert, Jakub Voznica, H       Morlon, Florian Hartig

Diversification Models

We chose two established diversification models as case studies to test the performance of deep learning algorithms for phylogenetic inference: 1) the relatively simple and homogeneous CRBD model, and 2) the more complex inhomogeneous BiSSE model. The rationale for choosing these two models was to have two models with tractable likelihoods but different complexity, and especially different in their (in)homogeneity, as we conjectured that homogenous BD will profit less from detailed representations of the phylogeny, given that it is known that all information for their inference is contained in the LTT.

The Constant Rate Birth-Death (CRBD) model is one of the simplest conceivable diversification models. It has two parameters, the speciation rate (λ) and the extinction rate (μ), that are homogeneously constant over time. The likelihood of this model is well-known (Nee et al., 1994) and depends only on the phylogeny's branching times and not on its topology. To estimate diversification rates with the MLE, we used the APE R package (Paradis et al. 2004).

In the Binary State Speciation and Extinction (BiSSE) model, lineages can alternate between two states (0 and 1), where each state has its own speciation and extinction rate. The switch through time between the two states translates character transitions (e.g. sexual to asexual reproduction) that can have an impact on diversification rates. The model has 6 parameters: 2 speciation rates (λ_0, λ_1), 2 extinction rates (μ_0, μ_1) and 2 two transition rates (q_{01} for transition $0 \rightarrow 1$; q_{10} for transition $1 \rightarrow 0$). As for the CRBD model, the likelihood of the BiSSE model can be computed (see Maddison et al., 2007). We imposed four constraints on the model to simplify inference, thus decreasing the number of free parameters from six to two.

DEEP LEARNING TO INFER PHYLOGENY PARAMETERS

The constraints are: 1) $\lambda_1 = 2\lambda_0$; 2) $\mu_0 = 0$; 3) $\mu_1 = 0$; 4) $q_{01} = q_{10}$. Constraint 1) ensures that states 0 and 1 have different speciation rates, 2) and 3) make the model pure birth, and 4) is an assumption of symmetry that makes the probabilities to switch from one state to another equal. Lambert et al. (2022) also used the CRBD model, and a less constrained version of BiSSE. Here we simplified the model to focus on the comparison of network architectures and data representation. To estimate diversification rates with the MLE, we used the Diversitree R package (FitzJohn 2012) and constrained the likelihood with the 4 constraints listed above.

To train the neural networks, we simulated 100,000 phylogenies for the CRBD model and 1,000,000 phylogenies for the BiSSE model using the Diversitree library (FitzJohn 2012) in R. We assumed complete sampling of the phylogenies. The latter assumption (no missing species) could be relaxed (Lambert et al. 2022), but here our focus is on the comparison between inference methods. For the CRBD model, we draw the underlying parameters as follows: 1) we draw uniformly λ in $[0.1, 1.0]$; 2) we draw uniformly the turnover rate ε in $[0, 0.9]$ from which we compute the extinction rate $\mu = \varepsilon\lambda \in [0, 0.9\lambda]$. By doing so, we avoid the critical case where $\lambda \leq \mu$ (*i.e.*, speciation rate is inferior to or equivalent to the extinction rate). For the BiSSE model, we took $\lambda_0 \in [0.1, 1.0]$ to stay in the same range as for the CRBD model and $q_{01} \in [0.01, 0.1]$ to ensure that one state is not overly represented compared to the other one.

264 *Phylogeny Representation*

265 Most of the considered deep learning architectures cannot process phylogenies
266 as inputs, but require reformatting the phylogenies into a more regular data structure.
267 Here, we explain all options that we considered (see also Fig. 1).

268 *Summary statistics.*— Arguably the most basic option is to represent the
269 phylogeny by a number of summary statistics. We used a set of 84 summary
270 statistics inspired from the set of (Saulnier et al. 2017). Those summary statistics can
271 be split into three groups:

- 272 1) 8 statistics related to phylogeny topology (e.g. ratio of the width over the depth
273 of the phylogeny);
- 274 2) 25 branch lengths statistics (e.g. median of all branch lengths);
- 275 3) 51 LTT statistics (binned LTT coordinates and LTT slopes).

276 The list of the summary statistics and the changes compared to (Saulnier et al. 2017)
277 are detailed in the Table S1 of the Appendix.

278 For the BiSSE model we use the ratio of the number of tips in state 1 over the
279 total number of tips as an additional summary statistic.

280 *Lineage Through Time (LTT).*— LTTs illustrate the increase in lineages over
281 time. For a phylogeny of n tips, the LTT is composed of $n-1$ points where each point
282 is defined by two coordinates: time (t , abscissa) and the number of lineages (N ,
283 ordinate). For a binary tree where each branching event results in two daughter
284 lineages, the LTT can be compressed to a 1-d array without loss of information, by
285 throwing away the number of lineages and keeping only the times of speciation
286 events.

DEEP LEARNING TO INFER PHYLOGENY PARAMETERS

Phylogeny encoding (CBLV).— Yet another alternative is to encode the phylogeny in a real-values vector of length $2n-1$ named the ‘Compact Bijective Ladderized Vector’ (‘CBLV’, see Voznica et al., 2022). Each value of the vector corresponds to one node (internal node or tip), thus there are n values for the n tips and $n-1$ values for the internal nodes $n-1$, which result in a vector of $2n-1$ values. The encoding is done in two steps: 1) phylogeny ladderization, and 2) phylogeny traversal. The principle of ladderization is to order each node’s children, such that the encoding is bijective (*i.e.*, one CBLV maps exactly to one phylogeny and reversely). Here we ladderized the phylogeny such that for each node the left child is the child which is further from the root. On the ladderized phylogeny, we perform an inorder traversal using a classical recursive algorithm. If the visited node is an internal node or the first tip is visited, its distance to the root is added to the vector. Otherwise, its distance from its parent node is added to the vector. Moreover, for the BiSSE model we add the n tip states to the vector. The tip states are ordered according to the phylogeny traversal. Note that in the original method from Voznica et al. (2022), the tip state information was added by adding one row to the distance vector, thus resulting in a two-row matrix (first row for distances, second row for tip states), while here we concatenate two 1-d vectors resulting in a 1-d vector. We found that this modification did not affect the results.

Phylogeny as a graph.— The main motivation for the previous CBLV encoding is to transform the phylogeny into a regular Euclidean format that can be easily processed by CNNs. The disadvantage, however, is that neighborhood relationships of the graph can be distorted in this process. Recent research in the field of machine learning suggests that in such a case, it is often better to train neural networks directly with the original graphs. This is done by so-called Graph Neural Networks or

Ismaël Lajaaïti, Sophia Lambert, Jakub Voznica, H  l  ne Morlon, Florian Hartig

GNNs, which extend the CNN idea to graphs. Here, we use the Pytorch Geometric framework (Fey and Lenssen 2019) and the GraphNeuralNetworks Julia package base on the Flux framework (Innes 2018) to represent the phylogeny as graph and train GNNs. We provide the GNN with the phylogeny's topology and 4 attributes per node: distance to the root and the lengths of the 3 edges linked to the node (1 incoming edge: $\text{parent} \rightarrow \text{node}$; 2 outgoing edges: $\text{node} \rightarrow \text{child}_1$ and $\text{node} \rightarrow \text{child}_2$). Moreover, for the BiSSE model we add as an attribute the tip states (0 or 1 for tips, -1 for nodes whose state is unknown).

Neural Network Architectures

For predicting model parameters from the formatted phylogenies, we considered four different neural network architectures: DNN, CNN RNN and GNN (see also Fig. 1). All architectures were built within the torch framework (Falbel and Luraschi 2019) in R, except GNNs which were built with Torch in Python because the PyTorch Geometric library (Fey and Lenssen, 2019) was needed for GNNs. Hyperparameter tuning for each architecture was performed by hand (see Appendix Tables S0-S5).

328

DEEP LEARNING TO INFER PHYLOGENY PARAMETERS

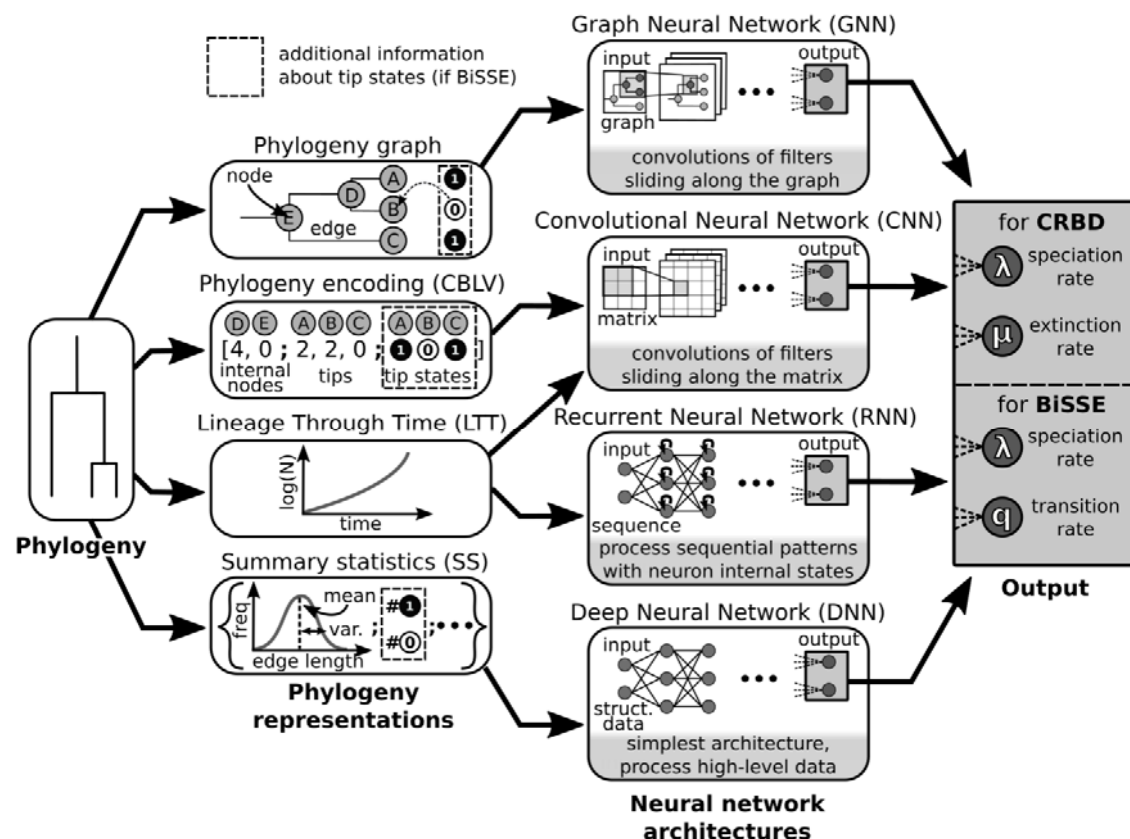


Figure 1. Combining phylogeny representations with neural network architectures. The five different combinations considered between phylogeny representations and neural network architectures are indicated by arrows from the first column to the second one. The rationales behind these five combinations are the following: 1) for phylogeny graph with GNN, GNN is the only architecture able to process graphs; 2) for CBLV with CNN, CNNs are able to detect patterns that are expected in the phylogeny encoding (Voznica et al. 2021); 3) for LTT with CNN, CNNs can detect patterns in the slope of the LTT; 4) for LTT with RNN, RNNs are designed to process time series; 5) SS with DNN, SS do not have spatial or temporal hierarchical order and therefore can be processed by a simple architecture. The third column describes the output of the inference methods for the two diversification models examined (CRBD and BiSSE).

Ismaël Lajaaïti, Sophia Lambert, Jakub Voznica, H       Morlon, Florian Hartig

Training Neural Networks

To train and validate the performance of the networks, we simulated 100,000 phylogenies under the CRBD model and 1,000,000 phylogenies under the BiSSE model. For both models phylogenies were split randomly in three groups: 1) a training set to train the neural networks (90% of the phylogenies); 2) a validation set used to quantify performance of the neural network during the training (5% of the phylogenies) and 3) a test set used to quantify the performance of the neural network after the training (5% of the phylogenies). These split sets were the same for all neural network architectures, so all of the architectures are trained and tested with the same phylogenies. Moreover, the Maximum Likelihood Estimation ('MLE') was tested on the phylogenies of the test set to fairly compare neural networks and MLE.

Training of the networks followed the standard practice of dividing the training data into small batches (typically 64 phylogenies per batch, for more details see the Appendix). During optimization, batches are successively provided to the network and its weights are adjusted to reduce the prediction error (defined as the mean squared error). Once the network has been fed with the whole training set, the weights are frozen and the performance of the network is evaluated on the validation set. This process of training and validation is called an 'epoch'. We repeated this process until the prediction error on the validation set stopped to improve (early stopping). This ensures that the network does not overfit the training data, which tends to improve the performance of the model on new data (Bengio 2012). In addition to early stopping, we also set at each new epoch a small proportion of the network weights to zero (dropout, set to 1%), another standard method to avoid overfitting. After the training of the networks, we evaluated their performances on the test set.

DEEP LEARNING TO INFER PHYLOGENY PARAMETERS

Interpreting Predictions Error

Once the neural networks were trained, we use them to infer the parameter values of the models from the test data (the phylogenies in the hold-out). We also calculated the Maximum Likelihood Estimate for these phylogenies to establish a baseline. Thus, for each method (the neural networks or the MLE) we have the predicted model parameters (y_{pred}) vs. the true values (y_{true}).

To better understand the origin of deviations between the true and predicted parameter values, we divide the prediction error into stochastic error and bias according to Theil coefficients (Smith and Rose 1995). The idea of this approach is that the sum squared differences $U_{tot} = \sum_{i=1}^n (y_{pred,i} - y_{true,i})^2$ can be expressed as a sum $U_{tot} = U_{uniformBias} + U_{consistencyBias} + U_{variance}$ where: 1) $U_{uniformBias} = n (\overline{y_{pred}} - \overline{y_{true}})^2$ corresponds the systematic error; 2) $U_{consistencyBias} = (b - 1)^2 \sum_{i=1}^n (y_{true,i} - \overline{y_{pred}})^2$ is the slope of the linear regression of y_{pred} vs. y_{true} and $\overline{y_{pred}}$ the mean of the predicted values; 3) $U_{variance} = \sum_{i=1}^n (y_{pred,i} - y_{pred,lm,i})^2$ is the stochastic error, measured by the variance of the y_{pred} around the regression slope $y_{pred,lm,i}$. Lastly, we normalize each term by the sum squared of the true parameter values: $U_d = \sum_{i=1}^n y_{true,i}^2$. The error decomposition is illustrated in Figure 2.

DEEP LEARNING TO INFER PHYLOGENY PARAMETERS

learn to not predict values outside the parameter space they have seen, whereas the Maximum Likelihood cannot do so. Thus, when estimating parameters close to the boundaries of the explored parameter space, the variance of the neural network predictions artificially decreases due to the specific set up of the phylogeny simulations.

RESULTS

Overall, we find that deep learning methods show good performances as they predict rates with an error comparable to MLE in most cases (Fig. 3). Some deep learning methods even outperformed MLE (CNN and RNN with LTTs for the CRBD model, see Fig. 3a,b). From theory, one would expect that lower total error of DL methods can be explained by the bias-variance trade-off, which allows DL methods to trade off bias against a lower total error (e.g. Pichler & Hartig, 2023). Looking at the decomposition of the error, however, we do not find that the deep-learning methods show greater bias than the MLE (e.g. DNN with SS vs. MLE for the CRBD model in Fig. 3a,b). The only notable exception to the good performance of the deep learning models was the GNN as well as the RNN and CNNs fed with the LTT for the BISSE model, which all performed notably poorer than the MLE.

Ismaël Lajaaïti, Sophia Lambert, Jakub Voznica, H  l  ne Morlon, Florian Hartig

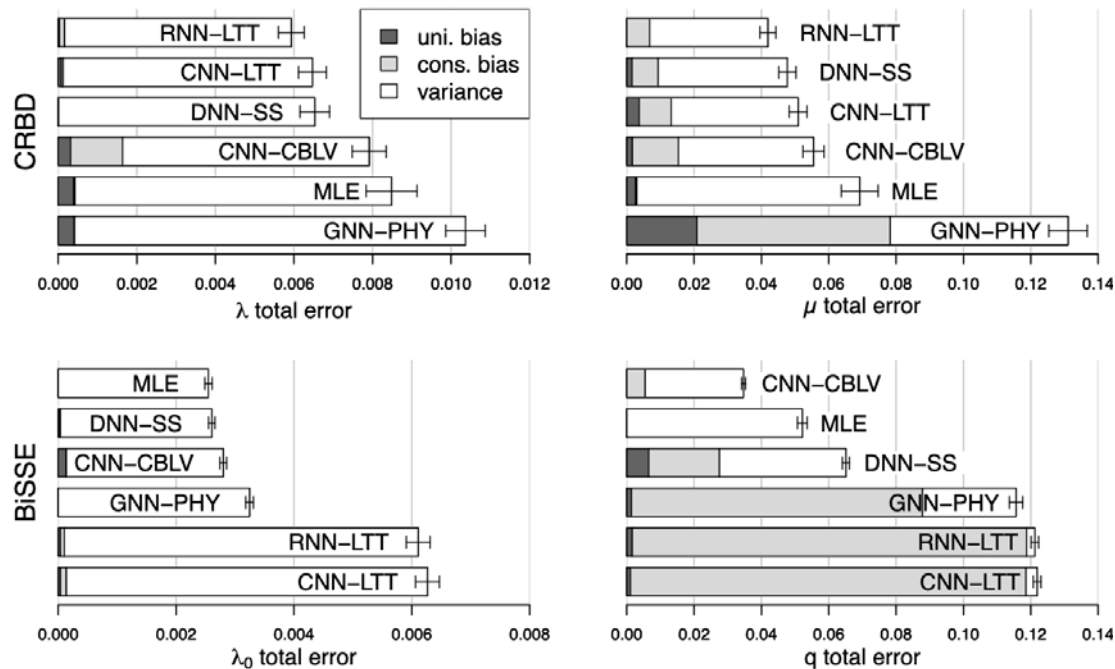


Figure 3. Prediction error of deep learning methods and MLE for the CRBD (a-b) and the BiSSE (c-d) model. From the CRBD we infer: a) the speciation rate (λ) and, b) the extinction rate (μ). From the BiSSE model we infer: c) the speciation rate of state 0 (λ_0) and, d) the transition rate (q), the other parameters are constrained (see Methods for more details). The deep learning methods evaluated are the following: DNN with summary statistics (DNN-SS), CNN with LTTs (CNN-LTT), RNN with LTTs (RNN-LTT), CNN with encoded phylogeny (CNN-CBLV) and GNN with phylogeny graphs (GNN-PHY). The dataset contains 100,000 phylogenies for the CRBD model and 1,000,000 for the BiSSE model. The total summed-squared error is split in three terms: variance, uniform bias and consistency bias (for more details see Fig. 2 or Smith and Rose 1995). The error bars correspond to the 95% confidence interval.

Our second question was to understand how the optimal phylogeny representation depends on the complexity of the underlying diversification model.

DEEP LEARNING TO INFER PHYLOGENY PARAMETERS

Our findings show that for the CRBD model, the best models are based on the LTT (CNN-LTT and RNN-LTT). Those models can even outperform the MLE (Fig. 3a,b). In contrast, inference methods relying on more complex phylogeny representations have a higher prediction error. This is especially clear for the two methods based on the most complex representations: CNN with full phylogeny encodings and GNN with phylogeny graphs. In sum, the more redundant information is added in the data, the worse the deep learning methods perform.

For the BiSSE model, we found a different behavior. CNN with encoded phylogenies and GNN with phylogeny graphs outperform simpler LTT-based models (Fig. 3). To understand which information is missing in the LTT and thus is responsible for the increased performance of the CNN with encoded phylogenies and GNN with phylogeny graphs compared to LTT-based models, we provided neural networks with data of more fine-grained increasing complexity. Specifically, we compared a CNN fed with LTTs as a baseline (1) with a CNN and three increasingly detailed encoded phylogenies (2-4). In the latter, we varied 2 features: the number of tip states and the location of tip states in the phylogeny. Thus, the 3 options are: excluding all tip states information (2); including information about the tip states, but not their location (3); including information about the tip states and their location (4; see Fig. 4c). To sum up, we compare 4 options: (1) no information about phylogeny's topology, tip state numbers and location, (2) information about topology but not about tip states, (3) information about phylogeny topology, tip state numbers but not about their location, and (4) information about phylogeny topology, tip state numbers and their location.

This analysis confirms that the LTT alone is insufficient to infer rates accurately, as can be seen by the CNN and RNN combined with LTTs being among the deep-

Ismaël Lajaaïti, Sophia Lambert, Jakub Voznica, H  l  ne Morlon, Florian Hartig

learning methods with the highest error (Fig. 3c,d). Moreover, the predictive
performance increases with each information that was added about tip states,
suggesting that each of the intermediate steps considered loses information (Fig. 4).

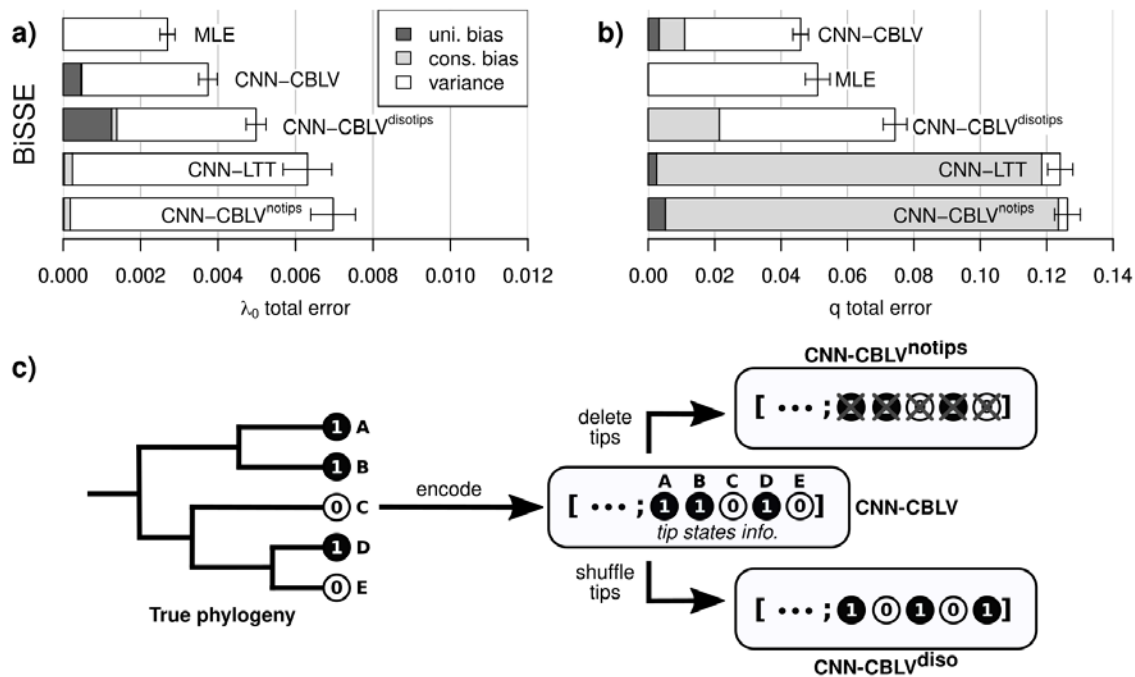


Figure 4. Prediction error of deep learning methods using different levels of tip states information for the BiSSE model. We infer: a) the speciation rate of state 0 (λ_0) and, b) the transition rate (q), the other parameters are constrained (see Methods for more details). c) The deep-learning methods evaluated are CNN with encoded phylogenies: excluding tip states information (CNN-CLBV^{notips}), containing tip states but randomly shuffled (CNN-CBLV^{disotips}), and containing tip states in order (CNN-CBLV) and are presented in panel c). Additionally, we consider CNN with LTT to have a reference of another deep learning method that does not use tip states information, and MLE which is our baseline. The dataset for training and testing neural networks contains 100,000 phylogenies. The total summed-squared error is

DEEP LEARNING TO INFER PHYLOGENY PARAMETERS

split in three terms: variance, uniform bias and consistency bias (for more details see Fig. 2). The error bars correspond to the 95% confidence interval.

When looking at the influence of the neural network architecture, we see that this choice interacts with the data representation: for simple data representations of the phylogeny, CNN and RNN combined with LTTs achieved a similar prediction accuracy in all cases (Fig. 3), and they were overall the best option for the CRBD model, whereas for the more complicated BISSE model, the even simpler DNN architecture with summary statistics outperformed the LTT-based architectures, whereas the CNN with encoded phylogenies performed best overall, including the MLE (Figs. 3, 4). The information provided to this architecture is equivalent, although differently structured, than the information provided to the GNN. The latter, however, performed notably poorer.

DISCUSSION

The goal of this study was to compare the ability of different deep learning architectures to infer parameters of diversification models from reconstructed phylogenies. Our main findings are that deep learning methods are surprisingly accurate for this task and can even outperform the MLE in some cases. Looking in more detail at the deep learning method, we find that the optimal phylogeny representation and network architecture depend on the diversification model. For the simple homogeneous CRBD model, we found that feeding the networks with the LTT was the main factor that improved inference, presumably because the LTT is a sufficient statistic and thus provides less redundant information to the networks. For the inhomogeneous BISSE model, it was optimal to provide the data in its most complex form, and the choice of the network architecture played a far greater role.

Ismaël Lajaaïti, Sophia Lambert, Jakub Voznica, H       Morlon, Florian Hartig

We speculate that these results will generalize: if simple sufficient statistics exist for a model, these should be used and the choice of the network architecture is likely secondary. If no simple sufficient data representation exists for a given model, more complicated network architectures have to be used, and the choice of the network architecture becomes more critical.

Note that, in line with these thoughts, the performance of the DNN with SS for the BISSE model might be improved by adding more informative summary statistics that encode tip state information. This idea is supported by our observation that predictions of CNNs with CBLV outperform predictions of DNN with SS for the transition rate by a great margin, suggesting that tip state information that are contained in the CBLV encoding is critical for the parameter inference.

Total Error and Bias

We ranked the different inference methods primarily by their total error, which sums up bias and variance (Smith and Rose 1995). This is in line with general practice in machine learning. To achieve a lower error, machine learning methods often trade off bias against variance (Pichler and Hartig 2023), whereas in statistics, bias is often seen as more crucial than variance, because an unbiased estimator allows a field to accumulate evidence over time (Shmueli 2010). Yet, given that there are usually no independent replicates of a phylogeny, we find it defensible to use the total error as the primary performance metric. Moreover, as we discuss below, DL algorithms did not generally exhibit larger bias than the MLE, suggesting that the problem of bias may be less severe than one might have anticipated.

Our results regarding total error on inferred parameters support earlier findings of (Voznica et al. 2022), who also reported that deep learning methods can outperform state-of-the-art methods when inferring model parameters from

DEEP LEARNING TO INFER PHYLOGENY PARAMETERS

phylogenies (BEAST 2 in his study, MLE in our study). Contrary to the general idea of the bias-variance trade-off expectations, we did not find that deep learning methods generate this performance advantage over the MLE by leveraging the bias-variance trade-off. Indeed, several deep learning methods often had a lower total error and a lower bias than MLE (where we expected that they traded off variance against a greater bias to achieve lower error). To explain these findings, we speculate that the MLE apparently also has some small-sample bias for the CRBD model, especially for low net diversification rates (*i.e.* $\mu \lesssim \lambda$).

Explaining the poor performance of the GNNs

Against our expectations, GNNs did not outperform other DL architectures and specifically the CNN with encoded phylogenies. This is surprising given the generally positive results in the machine learning literature about GNNs (Zhang et al. 2019), and the fact that GNNs are fed with the most accurate and natural representation of the data, which is the phylogeny itself. We speculate that our results can be explained by two well-known limitations of GNNs: ‘hop neighborhood’ (Nikolentzos et al. 2020) and ‘over-smoothing’ (Oono and Suzuki 2019).

First, ‘hop neighborhood’ refers to the fact that, in a GNN, at each new layer, node attributes are updated by aggregating their neighbor attributes (Scarselli et al. 2009). Thus, after k layers, each node aggregates only nodes that can be reached in k or less ‘hops’. Thus, node attributes only contain information about local graph structures but do not encode macroscopic graph information (Kriege et al. 2018). We speculate that for inhomogeneous birth-death models, the most important info about parameters related to the inhomogeneity is contained in subclades that have

Ismaël Lajaaiti, Sophia Lambert, Jakub Voznica, H  l  ne Morlon, Florian Hartig

diversified long ago, and thus typically have large graph distances. In such cases, the “short-sightedness” of GNNs might be a major limitation.

We tested to increase the number of GNN convolutional layers from 2 to 5 (for the exact architecture see Appendix Table S5-6) but it did not lead to a performance improvement. Indeed, the naïve way to counteract this limitation is to increase the number of GNN layers as the size of the ‘k-hop neighborhood’ increases with k the number of layers. However, by doing so one will encounter the second limitation: ‘over-smoothing’ (Oono and Suzuki 2019): when stacking many layers in a GNN, node attributes become indistinguishable from one another due to the cumulative aggregations occurring at each layer. This phenomenon is referred to as ‘over-smoothing’ (Li et al. 2018). Thus, adding layers in GNNs often results in a deterioration of predictive performances (Li et al., 2018).

The combination of the two latter limitations might explain why ‘classical’ GNNs failed to infer rates accurately from reconstructed phylogenies. We speculate that our results regarding GNNs could be improved by considering specific GNN variants designed to overcome these limitations (for over-smoothing see Li et al. 2019; and for hop neighborhood see Nikolentzos et al. 2020), and encourage further research in this direction.

Designing Efficient Deep-Learning Methods for Rate Inference

Our results reinforce previous analyses (Voznica et al. 2022; Lambert et al. 2022) suggesting that deep learning methods are a viable alternative to infer birth-death rates from phylogenetic data. This is particularly interesting for cases where likelihoods are not tractable or hard to compute. We refine these insights by demonstrating that the performance of the deep learning methods may strongly depend on data representation and network architecture. Regarding the complexity

DEEP LEARNING TO INFER PHYLOGENY PARAMETERS

of the phylogeny representation, we find that avoiding to provide redundant data seems to help the algorithms. For instance, for homogeneous models, the topology of the phylogeny does not influence the likelihood (Lambert and Stadler 2013). Thus, the LTT provides a less redundant representation of the phylogeny while still containing all information useful for the inference (sufficient statistic). For more complex diversification models, in particular for models with intractable likelihoods, it will likely be harder to find appropriate sufficient statistics, and deep learning methods that use the whole phylogeny might be needed. For the BiSSE model, we found that the fully encoded phylogeny (Voznica et al. 2022) containing phylogeny topology and tip states information was the best choice among the representations that we considered. In short, choosing a good representation of the data is important: over-complicated representation either costs unnecessary computational power or deteriorates the accuracy of the predictions for simple diversification models, while choosing an over-simplified representation for a complex diversification model may lead to poor predictions as the representation does not contain enough information to predict parameters properly.

Once a suitable phylogeny representation has been found, the appropriate neural network architecture has to be selected. First, the choice of the architecture is restricted by the data type e.g., a time series can go either with a CNN or an RNN but do not fit with a DNN which is not designed to detect patterns or to process temporal data. Secondly, the importance of the choice of the network architecture among the remaining possibilities is dependent on the complexity of the phylogeny representation: the more complex the representation, the more important the choice of the architecture is. In other words, when data become more difficult to process, more attention should be paid to the choice of the neural network architecture that

DEEP LEARNING TO INFER PHYLOGENY PARAMETERS

those would be likely still much larger and possibly less portable than current statistical procedures.

CONCLUSIONS

In conclusion, our study supports the idea that deep learning methods can be used to infer diversification rates from reconstructed phylogenies. In our results, they often showed similar and sometimes even better performance than the MLE. Thus, deep learning methods offer a promising approach to likelihood-based statistical inference, in particular for models whose likelihoods are intractable or hard to compute. However, our results also provide a warning that deep learning methods are very diverse and the choice of the method (*i.e.* the combination of a phylogeny representation and a neural network architecture) must be adjusted to the model considered. If that can be achieved, however, they may be instrumental in expanding our options to perform statistical inference for complicated macroevolutionary models.

CONFLICT OF INTEREST

The authors declare no conflict of interest.

SUPPLEMENTARY MATERIALS

The code to reproduce the results in this study is available at <https://github.com/ilajaaait/phylo-inference-ml>. Simulations data and the online appendix are available at <https://doi.org/10.5061/dryad.7h44i0zzq>.

ACKNOWLEDGEMENTS

We thank Maximilian Pichler and Sonia Kéfi for helpful discussions and comments on the manuscript. The design of our study profited from the results of a

Ismaël Lajaaïti, Sophia Lambert, Jakub Voznica, H  l  ne Morlon, Florian Hartig

645 MSc Thesis by Felix Gottschlich at the University of Regensburg that examined the
646 possibility to use GNNs for phylogenetic inference.

647

648

649

650 REFERENCES

651 Alfaro M.E., Santini F., Brock C., Alamillo H., Dornburg A., Rabosky D.L., Carnevale
652 G., Harmon L.J. 2009. Nine exceptional radiations plus high turnover explain
653 species diversity in jawed vertebrates. *Proc. Natl. Acad. Sci.* 106:13410–
654 13414.

655 Barnosky A.D., Matzke N., Tomiya S., Wogan G.O.U., Swartz B., Quental T.B.,
656 Marshall C., McGuire J.L., Lindsey E.L., Maguire K.C., Mersey B., Ferrer E.A.
657 2011. Has the Earth's sixth mass extinction already arrived? *Nature*. 471:51–
658 57.

659 Beaumont M.A. 2010. Approximate Bayesian Computation in Evolution and Ecology.
660 Annu. Rev. Ecol. Evol. Syst. 41:379–406.

661 Bengio Y. 2012. Neural Networks: Tricks of the Trade. Springer Berlin, Heidelberg.

662 Bukhari A.H., Raja M.A.Z., Sulaiman M., Islam S., Shoaib M., Kumam P. 2020.
663 Fractional Neuro-Sequential ARFIMA-LSTM for Financial Market Forecasting.
664 IEEE Access. 8:71326–71338.

665 Chan J., Perrohé V., Spence J.P., Jenkins P.A., Mathieson S., Song Y.S. 2018. A
666 Likelihood-Free Inference Framework for Population Genetic Data using
667 Exchangeable Neural Networks. *Adv. Neural Inf. Process. Syst.* 31:8594–
668 8605.

669 Condamine F.L., Rolland J., Morlon H. 2013. Macroevolutionary perspectives to
670 environmental change. *Ecol. Lett.* 16:72–85.

671 Csilléry K., Blum M.G.B., Gaggiotti O.E., François O. 2010. Approximate Bayesian
672 Computation (ABC) in practice. *Trends Ecol. Evol.* 25:410–418.

Etienne R.S., Haegeman B., Stadler T., Aze T., Pearson P.N., Purvis A., Phillimore
A.B. 2012. Diversity-dependence brings molecular phylogenies closer to
agreement with the fossil record. *Proc. R. Soc. B Biol. Sci.* 279:1300–1309.

Etienne R.S., Rosindell J. 2012. Prolonging the Past Counteracts the Pull of the Present: Protracted Speciation Can Explain Observed Slowdowns in Diversification. *Syst. Biol.* 61:204.

DEEP LEARNING TO INFER PHYLOGENY PARAMETERS

- 679 Falbel D., Luraschi. 2019. torch: Tensors and Neural Networks with “GPU”
680 Acceleration. Available from <https://torch.mlverse.org/docs/index.html>.
- 681 Fey M., Lenssen J.E. 2019. Fast Graph Representation Learning with PyTorch
682 Geometric. ArXiv190302428 Cs Stat.
- 683 FitzJohn R.G. 2012. Diversitree: comparative phylogenetic analyses of diversification
684 in R. *Methods Ecol. Evol.* 3:1084–1092.
- 685 G. E. Hutchison. 1959. Homage to Santa Rosalia or Why Are There So Many Kinds
686 of Animals? | *The American Naturalist*: Vol 93, No 870. Available from
687 <https://www.journals.uchicago.edu/doi/abs/10.1086/282070>.
- 688 Gaston K.J., Blackburn T.M. 2000. *Pattern and Process in Macroecology*. John
689 Wiley & Sons, Ltd.
- 690 Gilmer J., Schoenholz S.S., Riley P.F., Vinyals O., Dahl G.E. 2017. Neural Message
691 Passing for Quantum Chemistry. *Proc. 34th Int. Conf. Mach. Learn.*:1263–
692 1272.
- 693 Graves A., Fernández S., Schmidhuber J. 2005. Bidirectional LSTM Networks for
694 Improved Phoneme Classification and Recognition. *Artif. Neural Netw. Form.*
695 *Models Their Appl. – ICANN 2005.*:799–804.
- 696 Hagen O., Flück B., Fopp F., Cabral J.S., Hartig F., Pontarp M., Rangel T.F.,
697 Pellissier L. 2021. gen3sis: A general engine for eco-evolutionary simulations
698 of the processes that shape Earth’s biodiversity. *PLOS Biol.* 19:e3001340.
- 699 Hallinan N. 2012. The generalized time variable reconstructed birth–death process.
700 *J. Theor. Biol.* 300:265–276.
- 701 Hamilton W.L., Ying R., Leskovec J. 2018. Inductive Representation Learning on
702 Large Graphs. ArXiv170602216 Cs Stat.
- 703 Hartig F., Calabrese J.M., Reineking B., Wiegand T., Huth A. 2011. Statistical
704 inference for stochastic simulation models – theory and application. *Ecol. Lett.*
705 14:816–827.
- 706 Hillebrand H. 2004. On the Generality of the Latitudinal Diversity Gradient. *Am. Nat.*
707 163:192–211.
- 708 Hochreiter S., Schmidhuber J. 1997. Long Short-Term Memory. *Neural Comput.*
709 9:1735–1780.
- 710 Huang L., Ma D., Li S., Zhang X., Wang H. 2019. Text Level Graph Neural Network
711 for Text Classification. .
- 712 Innes M. 2018. Flux: Elegant machine learning with Julia. *J. Open Source Softw.*
713 3:602.
- 714 Kipf T.N., Welling M. 2017. Semi-Supervised Classification with Graph Convolutional
715 Networks. ArXiv160902907 Cs Stat.

Ismaël Lajaaïti, Sophia Lambert, Jakub Voznica, H       Morlon, Florian Hartig

- 716 Kriege N.M., Morris C., Rey A., Sohler C. 2018. A Property Testing Framework for
717 the Theoretical Expressivity of Graph Kernels. Proc. Twenty-Seventh Int. Jt.
718 Conf. Artif. Intell.:2348–2354.
- 719 Lambert A., Stadler T. 2013. Birth–death models and coalescent point processes:
720 The shape and probability of reconstructed phylogenies. Theor. Popul. Biol.
721 90:113–128.
- 722 Lambert S., Voznica J., Morlon H. 2022. Deep Learning from Phylogenies for
723 Diversification Analyses. :2022.09.27.509667.
- 724 LeCun Y., Bengio Y., Hinton G. 2015. Deep learning. Nature. 521:436–444.
- 725 Li G., Muller M., Thabet A., Ghanem B. 2019. DeepGCNs: Can GCNs Go As Deep
726 As CNNs? :9267–9276.
- 727 Li Q., Han Z., Wu X.-M. 2018. Deeper Insights into Graph Convolutional Networks
728 for Semi-Supervised Learning. .
- 729 Louca S., Pennell M.W. 2020. Extant timetrees are consistent with a myriad of
730 diversification histories. Nature. 580:502–505.
- 731 Maddison W.P., Midford P.E., Otto S.P. 2007. Estimating a Binary Character’s Effect
732 on Speciation and Extinction. Syst. Biol. 56:701–710.
- 733 Maliet O., Hartig F., Morlon H. 2019. A model with many small shifts for estimating
734 species-specific diversification rates. Nat. Ecol. Evol. 3:1086–1092.
- 735 Mansimov E., Mahmood O., Kang S., Cho K. 2019. Molecular Geometry Prediction
736 using a Deep Generative Graph Neural Network. Sci. Rep. 9:20381.
- 737 Mittelbach G.G., Schemske D.W., Cornell H.V., Allen A.P., Brown J.M., Bush M.B.,
738 Harrison S.P., Hurlbert A.H., Knowlton N., Lessios H.A., McCain C.M.,
739 McCune A.R., McDade L.A., McPeck M.A., Near T.J., Price T.D., Ricklefs
740 R.E., Roy K., Sax D.F., Schluter D., Sobel J.M., Turelli M. 2007. Evolution and
741 the latitudinal diversity gradient: speciation, extinction and biogeography.
742 Ecol. Lett. 10:315–331.
- 743 Moen D., Morlon H. 2014. Why does diversification slow down? Trends Ecol. Evol.
744 29:190–197.
- 745 Morlon H. 2014. Phylogenetic approaches for studying diversification. Ecol. Lett.
746 17:508–525.
- 747 Morlon H., Parsons T.L., Plotkin J.B. 2011. Reconciling molecular phylogenies with
748 the fossil record. Proc. Natl. Acad. Sci. 108:16327–16332.
- 749 Morlon H., Robin S., Hartig F. 2022. Studying speciation and extinction dynamics
750 from phylogenies: addressing identifiability issues. Trends Ecol. Evol.

DEEP LEARNING TO INFER PHYLOGENY PARAMETERS

- 751 Nee S., Holmes E.C., May R.M., Harvey P.H., Lawton J.H., May R.M. 1994.
752 Extinction rates can be estimated from molecular phylogenies. *Philos. Trans.*
753 *R. Soc. Lond. B. Biol. Sci.* 344:77–82.
- 754 Nikolettos G., Dasoulas G., Vazirgiannis M. 2020. k-hop graph neural networks.
755 *Neural Netw.* 130:195–205.
- 756 Oono K., Suzuki T. 2019. Graph Neural Networks Exponentially Lose Expressive
757 Power for Node Classification. .
- 758 Paradis E., Claude J., Strimmer K. 2004. APE: Analyses of Phylogenetics and
759 Evolution in R language. *Bioinformatics.* 20:289–290.
- 760 Pichler M., Hartig F. 2023. Machine learning and deep learning—A review for
761 ecologists. *Methods Ecol. Evol.* n/a.
- 762 Pontarp M., Bunnefeld L., Cabral J.S., Etienne R.S., Fritz S.A., Gillespie R., Graham
763 C.H., Hagen O., Hartig F., Huang S., Jansson R., Maliet O., Münkemüller T.,
764 Pellissier L., Rangel T.F., Storch D., Wiegand T., Hurlbert A.H. 2019. The
765 Latitudinal Diversity Gradient: Novel Understanding through Mechanistic Eco-
766 evolutionary Models. *Trends Ecol. Evol.* 34:211–223.
- 767 Pyron R.A., Burbrink F.T. 2013. Phylogenetic estimates of speciation and extinction
768 rates for testing ecological and evolutionary hypotheses. *Trends Ecol. Evol.*
769 28:729–736.
- 770 Rabosky D.L. 2009a. Ecological limits and diversification rate: alternative paradigms
771 to explain the variation in species richness among clades and regions. *Ecol.*
772 *Lett.* 12:735–743.
- 773 Rabosky D.L. 2009b. Heritability of Extinction Rates Links Diversification Patterns in
774 Molecular Phylogenies and Fossils. *Syst. Biol.* 58:629–640.
- 775 Rabosky D.L., Lovette I.J. 2008. Explosive Evolutionary Radiations: Decreasing
776 Speciation or Increasing Extinction Through Time? *Evolution.* 62:1866–1875.
- 777 Ricklefs R.E. 2007. Estimating diversification rates from phylogenetic information.
778 *Trends Ecol. Evol.* 22:601–610.
- 779 Rolland J., Condamine F.L., Jiguet F., Morlon H. 2014. Faster Speciation and
780 Reduced Extinction in the Tropics Contribute to the Mammalian Latitudinal
781 Diversity Gradient. *PLOS Biol.* 12:e1001775.
- 782 Saulnier E., Gascuel O., Alizon S. 2017. Inferring epidemiological parameters from
783 phylogenies using regression-ABC: A comparative study. *PLOS Comput. Biol.*
784 13:e1005416.
- 785 Scarselli F., Gori M., Tsoi A.C., Hagenbuchner M., Monfardini G. 2009. The Graph
786 Neural Network Model. *IEEE Trans. Neural Netw.* 20:61–80.
- 787 Schrider D.R., Kern A.D. 2018. Supervised Machine Learning for Population
788 Genetics: A New Paradigm. *Trends Genet.* 34:301–312.

Ismaël Lajaaïti, Sophia Lambert, Jakub Voznica, H       Morlon, Florian Hartig

789 Shmueli G. 2010. To Explain or to Predict? *Stat. Sci.* 25:289–310.

790 Silvestro D., Schnitzler J., Zizka G. 2011. A Bayesian framework to estimate
791 diversification rates and their variation through time and space. *BMC Evol.*
792 *Biol.* 11:311.

793 Smith E.P., Rose K.A. 1995. Model goodness-of-fit analysis using regression and
794 related techniques. *Ecol. Model.* 77:49–64.

795 Stadler T. 2011. Mammalian phylogeny reveals recent diversification rate shifts.
796 *Proc. Natl. Acad. Sci.* 108:6187–6192.

797 Stadler T. 2013. Recovering speciation and extinction dynamics based on
798 phylogenies. *J. Evol. Biol.* 26:1203–1219.

799 Voznica J., Zhukova A., Boskova V., Saulnier E., Lemoine F., Moslonka-Lefebvre M.,
800 Gascuel O. 2021. Deep learning from phylogenies to uncover the
801 transmission dynamics of epidemics. :2021.03.11.435006.

802 Voznica J., Zhukova A., Boskova V., Saulnier E., Lemoine F., Moslonka-Lefebvre M.,
803 Gascuel O. 2022. Deep learning from phylogenies to uncover the
804 epidemiological dynamics of outbreaks. *Nat. Commun.* 13:3896.

805 Wu Z., Pan S., Chen F., Long G., Zhang C., Yu P.S. 2021. A Comprehensive Survey
806 on Graph Neural Networks. *IEEE Trans. Neural Netw. Learn. Syst.* 32:4–24.

807 Yu Y., Si X., Hu C., Zhang J. 2019. A Review of Recurrent Neural Networks: LSTM
808 Cells and Network Architectures. *Neural Comput.* 31:1235–1270.

809 Zhang S., Tong H., Xu J., Maciejewski R. 2019. Graph convolutional networks: a
810 comprehensive review. *Comput. Soc. Netw.* 6:11.

811

812

DEEP LEARNING TO INFER PHYLOGENY PARAMETERS